Synthetic Peptidyl–tRNA Analogues

Amphiphilic 3′-Peptidyl-RNA Conjugates**

*Silvia Terenzi, Ewa Biała, Nhat Quang Nguyen-Trung, and Peter Strazewski**

The crystal structure of the large ribosomal subunit at nearly atomic resolution determined by Steitz and co-workers constitutes a milestone for the elucidation of the molecular basis of protein synthesis.[1] So far, only analogues of aminoacyl-tRNAs[1b,2] and in vitro-synthesized peptidyl-tRNAs[3,4] have been used in X-ray crystallographic, chemical footprinting, and cryo-electron microscopic structural investigations.

Herein we describe the synthesis and characterization of the first synthetic peptidyl–tRNA analogues, whose structural features should render them suitable for a cocrystallization with the large ribosomal subunit. In contrast to native peptidyl-tRNAs bearing a readily hydrolysable ester linkage between the nascent peptide and the tRNA, we have designed analogues in which the peptide is linked through a stable amide bond.

Our immediate goal, however, is to study the supramolecular aggregation properties of amphiphilic peptidyl-RNA conjugates that are likely to have played an important role at the origin of RNA-controlled peptide synthesis. Largely lipophilic peptides with a well defined secondary structure and appropriate length[5] might have been advantageous in a hypothetical "RNA world", as they could have served as molecular "anchoring devices" that would enable their RNA carriers to be transiently immobilized, compartmentalized, and thus highly concentrated on or in spheroidal lipidic bilayer vesicles, as proposed in the literature.[6] It seems to us of particular interest to investigate such systems experimentally by using synthetic, well-defined model systems, to test, for instance, if and how one could control the direction of RNA insertion into lipidic bilayer vesicles ("RNA-outside" versus "RNA-inside"). Besides, highly amphiphilic macromolecules bear the potential of unexpected material properties that could be exploited in various ways.

The RNA part of our conjugates consists of a 22-mer oligoribonucleotide hairpin mimicking the acceptor stem of *Escherichia coli* $tRNA^{Ala}$ closed by a stable UUCG tetraloop and peptidylated at its 3′-terminal single-stranded overhang, the so-called CCA terminus of tRNAs (Figure 1).

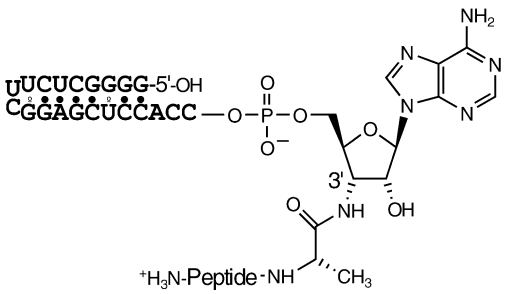

Figure 1. General structure of our 3′-peptidyl-RNA conjugates mimicking the acceptor stem peptidyl-$tRNA^{Ala}$.

Alanine and glutamic acid residues—early prebiotic amino acids—were chosen as the constituents of the oligopeptides. The length of the oligoalanine-based peptides—some with interdispersed or *N*-terminal glutamate residues to modulate their lipophilicity—varies between 8 and 22 amino acids (an α-helix of approximatively 20 amino acids suffices to span a lipidic bilayer). Their sequences are listed in Table 1.

[*] Prof. Dr. P. Strazewski
Laboratoire de Synthèse de Biomolécules
Bâtiment Eugène Chevreul (5ème étage)
Univerisité Claude Bernard - Lyon 1
Domaine Scientifique de la Doua
43 boulevard du 11 novembre 1918, 69622 Villeurbanne Cedex (France)
Fax: (+33) 4-7243-1323
E-mail: peter.strazewski@unibas.ch
S. Terenzi, N. Q. Nguyen-Trung
Institute of Organic Chemistry
University Basel
St. Johanns-Ring 19, 4056 Basel (Switzerland)
Dr. E. Biała
Institute of Bioorganic Chemistry
Polish Academy of Sciences
Noskowskiego 12/14, 61-704 Poznań (Poland)

[**] This work was supported by the Swiss National Science Foundation and the Novartis Foundation. We thank Profs. Paul Jenö and Thomas Kiefhaber, Biocentre, University of Basel, for making available their, respectively, MALDI-ToF and CD spectrometer facilities. We thank Drs. Anthony Coleman and Patrick Shahgaldian, Institut de Biologie et Chimie de Proteines (IBCP), Lyon, for carrying out and analyzing the DLS and AFM measurements.

Supporting information for this article is available on the WWW under http://www.angewandte.org or from the author.

 DOI: 10.1002/ange.200350926

Table 1: Peptide sequences of 3′-peptidyl-RNA.

Conjugate	Sequence
4a	$^{-}O_3PO$-5′-RNA-3′-$(Ala)_8$
4b	HO-5′- RNA-3′-$(Ala)_{16}$
4c	HO-5′- RNA-3′-$(Ala)_{10}Glu$
4d[a]	HO-5′- RNA-3′-$(Ala)_{18}(Glu)_2pGlu$
4e	HO-5′- RNA-3′-$(Ala)_7Glu(Ala)_7Glu(Ala)_4(Glu)_2$
4f	HO-5′- RNA-3′-$(Ala)_{20-22}$

[a] The amino-terminal pyroglutamate was probably formed during the purification steps.

The first building block was the orthogonally protected derivative **1** of 3′-alanylamino-3′-deoxyadenosine[7] immobilized on a suitable resin (Scheme 1). A relatively low loading of the resin was anticipated in view of the fact that we wished to synthesize long oligoalanine stretches that are in danger of aggregating at too high loadings[8] (in situ β-sheet formation), which could jeopardize the overall yields. To avoid undesired ester aminolyses of glutamate side chains that, during the final deprotection with methyl amine, might have generated N^{δ}-methyl glutamines, the glutamic acid side chains were protected as allyl esters, which were cleaved on the solid support before treatment with methyl amine.[9] After completion of the stepwise oligopeptide and then oligoribonucleotide synthesis, the crude conjugates were deprotected and detached from the solid support (by using methyl amine), desilylated, purified by HPLC, and identified by MALDI-ToF mass spectrometry.

The secondary structures of the RNA hairpin and the peptidic moieties were studied by CD spectroscopy at 0, 25, and 60 °C. Under the conditions used the peptide-free RNA hairpin exhibits a T_m value of 87.6 °C and is completely folded (stable A_{260} baseline) up to ≈60 °C.[10] CD spectra at 0 °C (Figure 2; 25 and 60 °C: see Supporting Information) show a strong positive Cotton effect between 245 and 295 nm that originates from the nucleotidic part only. All the conjugates analyzed show a more intense signal at Θ_{270} as compared to the hairpin alone (**4a:** +13%, **4d**: +42%), thus indicating that the single-stranded CCA-terminus of the hairpin, quite free to move when no peptide is present, is rigidified when a peptide is bonded to it. Moreover, the rigidification seems to roughly correlate with the degree of the predicted helicity of the peptide (AGADIR[11]).

The peptidic part induces an additional negative Cotton Effect in the region between 200 and 240 nm. The difference spectra between the peptide-free RNA hairpin and the conjugates (Figure 3) give evidence for the conformation adopted by the RNA-bound peptides in solution.

The negative bands at ≈208 and ≈222 nm are characteristic of α-helical peptides. A helical secondary structure is clearly adopted by **4b**, **4d** and **4e**, whereas **4a**, which has only eight alanines and thus should be predominantly random-coil, does not show the two bands. The degrees of helicity of the peptides were not quantified from the difference spectra because minor contributions to the negative Cotton effect arising from the differential changes originating from the RNA part of the conjugates (with a minimum at 211 nm) can neither be excluded nor determined.

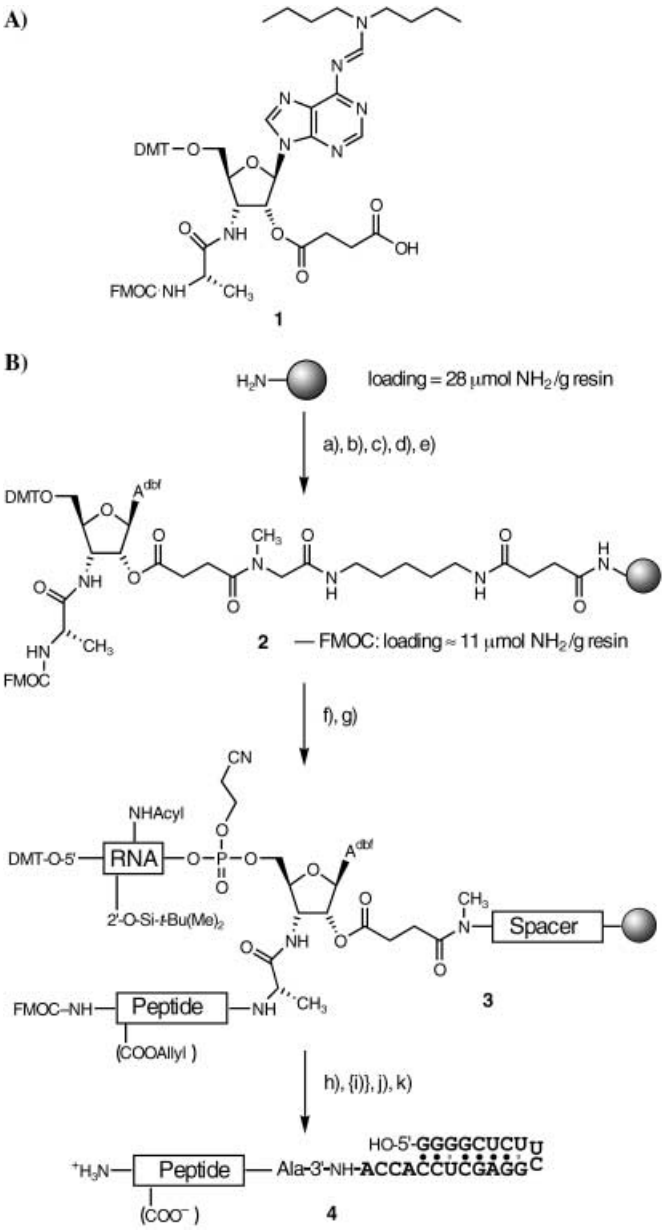

Scheme 1. A) Building block for the synthesis of 3′-peptidyl-RNA. B) Synthesis of the conjugates: a) 1. aminomethyl polystyrene 50% crosslinked with *p*-divinyl benzene, succinic anhydride, DMAP; 2. Ac_2O, pyridine, NMI, DMF; b) 1. Oxalyl chloride, CH_2Cl_2; 2. 1,6-diaminohexane, DMAP, CH_2Cl_2; c) BOC-Sarcosine, HBTU, NMM, DMF; d) 1. TFA/CH_2Cl_2; 2. Et_3N/DMF; e) 1. Building block **1**, HATU, NMM, DMF; 2. Ac_2O, pyridine, NMI, DMF. The loadings were determined by using the quantitative ninhydrin test. f) FMOC-based peptide synthesis, FMOC-amino acid + DEPBT; g) phosphoramidite-based RNA synthesis; h) 3% TCA in CH_2Cl_2; i) 1. $Pd(PPh_3)_4$, $PhSiH_3$, CH_2Cl_2; 2. $NH_4^+Et_2NCS_2^-$/DMF}; j) 38% CH_3NH_2 in EtOH/H_2O (1:1), 2 h, RT; k) $Et_3N{\cdot}3HF$, DMF, 1.5 h, 65 °C; *n*-butanol, −20 °C; SAX- and RP-HPLC. Abbrev.: BOC = *tert*-butoxycarbonyl; dbf = *N*,*N*-di-n-butylformamidine; DEPBT = 3-(diethoxyphosphoryloxy)-1,2,3-benzotriazin-4(3*H*)-one; DMT = *p*,*p*-dimethoxytriphenylmethyl ("dimethoxytrityl"); FMOC = 9-fluorenylmethoxycarbonyl; HATU = *O*-(7-azabenzotriazol-1-yl)-*N*,*N*,*N*′,*N*′-tetramethyluronium hexafluorophosphate; HBTU = *O*-(benzotriazol-1-yl)-*N*,*N*,*N*′,*N*′-tetramethyluronium hexafluorophosphate; NMI = *N*-methylimidazole; NMM = *N*-methylmorpholine; TCA = trichloroacetic acid; TFA = trifluoroacetic acid.

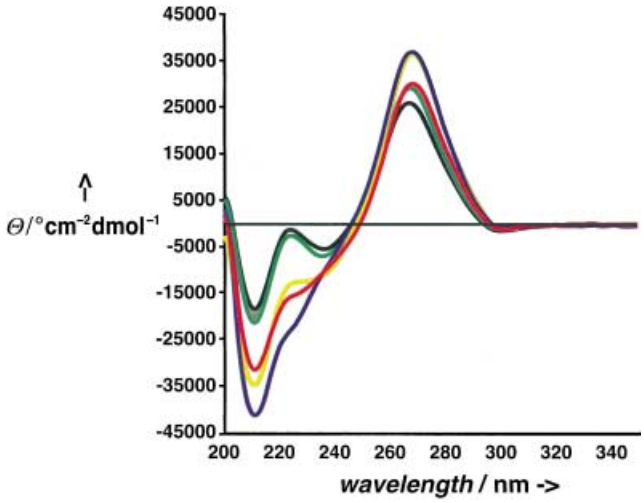

Figure 2. CD spectra of a ≈2.4 μM solution ($A_{260nm,25°C} \approx 0.35$, $\varepsilon_{260,calcd} = 145\,100\ M^{-1}cm^{-1}$, 100 mM NaCl, 10 mM $Na_xH_yPO_4$, pH 7.5) of the conjugates **4a** (green), **4b** (yellow), **4d** (blue), **4e** (red) and the unpeptidylated RNA hairpin × (black) taken at 0°C and normalized for the number of nucleotide residues. A strong and a weak negative Cotton Effect at 211 nm and 236 nm, respectively, and a positive one at 266 nm (black line) are typical for the A conformation of double-stranded RNA.

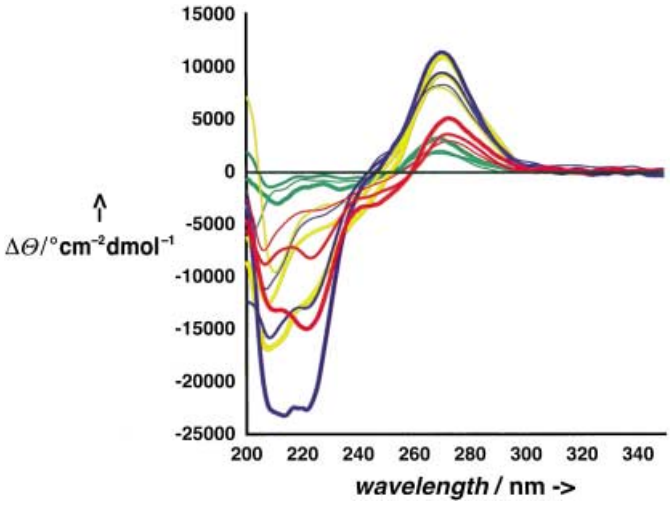

Figure 3. Difference CD spectra (**4a**,**b**,**d**,**e** minus x; see legend of Figure 2 for color scheme) at 0 (thick lines), 25 (normal lines) and 60°C (thin lines), normalized as in Figure 2. Note how the nucleobase region $\Theta_{245-295}$ withstands heat denaturation more than the peptide region $\Theta_{200-240}$, and that Θ_{222} denatures more readily than Θ_{208} at elevated temperatures.[15]

Furthermore, we measured the thermal denaturation profiles of the conjugates **4a–e** between 20 and 102°C at 260 nm (only RNA denaturation observed) and compared them to those of the parent unpeptidylated RNA hairpin, the RNA hairpin bearing a 5′-phosphate, a 3′-alanine, or both. The profiles and corresponding full thermodynamic parameters are shown in the Supporting Information. Briefly, no major influence on the thermodynamic stability of the RNA hairpins is observed in any of the examined conjugates (T_m values: 87.7–88.8°C). However, the presence of a peptide renders the RNA hairpin transition significantly shallower, a statistical effect and strong indication for a higher molecularity of the melting process.[12] Denaturation molecularities higher than one, in turn, are a first indication that our amphiphilic conjugates do show a tendency to aggregate in diluted aqueous solutions, a property that is not observed at all in the denaturation profiles of the unpeptidylated RNA hairpins.

Preliminary dynamic light scattering (DLS) and atomic force microscopy (AFM) studies confirm the above conclusion. Conjugate **4f** forms highly polydisperse aggregates in aqueous solution (size distribution between 80 nm and 1 μm with an abundance peak at 428 nm and an abundance shoulder at around 150 nm, as determined by DLS) which, when deposited on a glass surface and air-dried, form nanovesicles of a much narrower size distribution (Figure 4). DLS and AFM control experiments showed that

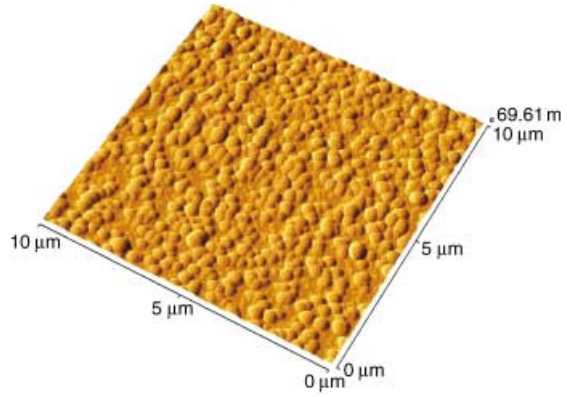

Figure 4. AFM scan over an air-dried solution of conjugate **4f** on a glass plate. Average size of the vesicles (50 vesicles analyzed): $h\varnothing = 13 \times 204$ nm. Polydispersity: $h\varnothing = 2 \times 102–36 \times 380$ nm. Height-diameter ratios: $100h/\varnothing = 2.0–9.5\,\%$, average 5.8%.

the unpeptidylated RNA hairpin, as expected, does not self-assemble in solution, nor does it form vesicles on a surface; when a highly concentrated RNA-hairpin solution was air-dried on a glass plate it instead formed microcrystals of 10–40 μm length (not shown). These observations confirm that amphiphilic constructs containing a hydrophilic RNA hairpin and a hydrophobic α-helical oligopeptide moiety of similar lengths, estimated to be together 9–10 nm long and ≤0.2 nm thick, indeed bear the potential of spontaneous self-assemblage into higher-order structures, even in the absence of lipids.

In conclusion, we have demonstrated the synthetic feasibility of amphiphilic conjugates mimicking peptidyl-tRNA. In the literature many examples of the synthesis of oligo(nucleotide-peptide) conjugates are present that follow two different synthetic strategies: fragment coupling[13] or the stepwise total-synthesis approach.[14] Our conjugates have been synthesized by following the second approach and, to the best of our knowledge, these are the only examples with an oligopeptide directly bonded in a biomimetic (and spacer-free) way to the 3′ terminus of an oligoribonucleotide. We believe that the methodology presented herein is powerful

and versatile and should be applicable to the stepwise synthesis of many different oligo(ribonucleotide-peptide) conjugates. Our conjugates could open the way to new constructs which might be able to form higher-order assemblies with unexpected properties.

Received: January 13, 2003
Revised: March 24, 2003 [Z50926]

Keywords: amphiphiles · bioorganic chemistry · nucleotides · peptides · self-assembly

[1] a) N. Ban, P. Nissen, J. Hansen, P. B. Moore, T. A. Steitz, *Science* **2000**, *289*, 905; b) P. Nissen, N. Ban, J. Hansen, P. B. Moore, T. A. Steitz, *Science* **2000**, *289*, 920.
[2] a) R. K. Agrawal, A. B. Heagle, P. Penczek, R. A. Grassucci, J. Frank, *Nat. Struct. Biol.* **1999**, *6*, 643; b) H. Stark, M. V. Rodnina, H.-J. Wieden, M. van Heel, W. Wintermeyer, *Cell* **2000**, *100*, 301.
[3] a) K. Stade, S. Riens, D. Bochkariov, R. Brimacombe, *Nucleic Acids Res.* **1994**, *22*, 1394; b) K. M. Choi, R. Brimacombe, *Nucleic Acids Res.* **1998**, *26*, 887.
[4] R. Beckmann, C. M. T. Spahn, N. Eswar, J. Helmers, P. A. Penczek, A. Sali, J. Frank, G. Blobel, *Cell* **2001**, *107*, 361.
[5] A. Percot, X. X. Zhu, M. Lafleur, *Biopolymers* **1999**, *50*, 647.
[6] T. Cavalier-Smith, *J. Mol. Evol.* **2001**, *53*, 555.
[7] a) O. Botta, P. Strazewski, *Nucleosides Nucleotides* **1999**, *18*, 721; b) N. Q. Nguyen-Trung, O. Botta, S. Terenzi, P. Strazewski, *J. Org. Chem.* **2003**, *68*, 2038.
[8] R. Warras, J.-M. Wieruszeski, C. Boutillon, G. Lippens, *J. Am. Chem. Soc.* **2000**, *122*, 1789.
[9] a) Y. Hayakawa, S. Wakabayashi, H. Kato, R. Noyori, *J. Am. Chem. Soc.* **1990**, *112*, 1691; b) N. Thieret, F. Guibé, F. Albericio, *Org. Lett.* **2000**, *2*, 1815.
[10] a) P. Strazewski, E. Biała, K. Gabriel, W. H. McClain, *RNA* **1999**, *5*, 1490; b) E. Biała, P. Strazewski, *J. Am. Chem. Soc.* **2002**, *124*, 3540.
[11] V. Muñoz, L. Serrano *J. Mol. Biol.* **1994**, *245*, 275: http://www.embl-heidelberg.de/Services/serrano/agadir/agadir-start.html.
[12] A. Dorenbeck, M. Scheffler, M. Wüstefeld, G. von Kiedrowski, *Angew. Chem./Angew. Chem. Int. Ed.* **2003**, in press.
[13] a) T. S. Zatsepin, D. A. Stetsenko, A. A. Arzumanov, E. A. Romanova, M. J. Gait, T. S. Oretskaya, *Bioconjugate Chem.* **2002**, *13*, 822; b) D. Forget, D. Boturyn, E. Defrancq, J. Lhomme, P. Dumy, *Chem. Eur. J.* **2001**, *7*, 3976; c) D. A. Stetsenko, M. J. Gait, *J. Org. Chem.* **2000**, *65*, 4900; d) M. McPherson, M. C. Wright, P. A. Lohse, *Synlett* **1999**, 978; e) D. L. McMinn, M. M. Greenberg, *J. Am. Chem. Soc.* **1998**, *120*, 3289; f) S. Soukchareun, J. Haralambidis, G. Tregear, *Bioconjugate Chem.* **1998**, *9*, 466; g) J. G. Harrison, S. Balasubramanian, *Nucleic Acids Res.* **1998**, *26*, 3136.
[14] a) Z. J. Gartner, M. W. Kanan, D. R. Liu, *J. Am. Chem. Soc.* **2002**, *124*, 10304; b) M. Antopolsky, E. Azhayeva, U. Tengvall, A. Azhayev, *Tetrahedron Lett.* **2002**, *43*, 527; c) D. A. Stetsenko, M. J. Gait, *Bioconjugate Chem.* **2001**, *12*, 576; d) M. de Champdoré, L. De Napoli, G. Di Fabio, A. Messere, D. Montesarchio, G. Piccialli, *Chem. Commun.* **2001**, 2598; e) V. Marchán, C. Rodríguez-Tanty, M. Estrada, E. Pedroso, A. Grandas, *Eur. J. Org. Chem.* **2000**, 2495; f) B. García de la Torre, F. Albericio, E. Saison-Behmoaras, A. Bachi, R. Eritja, *Bioconjugate Chem.* **1999**, *10*, 1005; g) I. Schwope, C. F. Bleczinski, C. Richert, *J. Org. Chem.* **1999**, *64*, 4749; h) F. Bergmann, W. Bannwarth, *Tetrahedron Lett.* **1995**, *36*, 1839.
[15] P. Wallimann, R. J. Kennedy, J. S. Miller, W. Shalongo, D. S. Kemp, *J. Am. Chem. Soc.* **2003**, *125*, 1203.

